CLM - R 39

United Kingdom Atomic Energy Authority

RESEARCH GROUP

Report

DETECTION OF AN ELECTRON BEAM IN A TOROIDAL PLASMA

D. W. ATKINSON
J. M. S. SCHOFIELD

Culham Laboratory,

Culham, Abingdon, Berkshire

1965

Available from H. M. Stationery Office

THREE SHILLINGS NET

U.D.C.
533.9.082.74
533.922

UNCLASSIFIED
(Approved for Sale)

CLM - R 39

DETECTION OF AN ELECTRON BEAM IN A TOROIDAL PLASMA

by

D.W. ATKINSON
J.M.S. SCHOFIELD

A B S T R A C T

Two methods are described for measuring the energy and flux of an electron beam which is immersed in a high density plasma in a toroidal magnetic field when the beam energy is only a few kilovolts. The first method uses an X-ray technique which enables the mean energy of the beam to be measured directly provided the spread is small. The spectrum of X-rays emitted from a tungsten target in the path of the beam is analysed with two or more scintillation counters and the energy and flux calculated from previous calibrations. A sufficiently monoenergetic beam whose energy is varied over the required range, is used to calibrate the system. Total energy is measured because the determination does not depend strongly on the angle of the beam velocity to the magnetic field. The second method measures the energy of the beam along the magnetic field only. The electrons are retarded by the potential of a planar grid. Those electrons with sufficient energy to be transmitted are collected and measured. The grid potential is pulsed on for two microseconds, which gives insufficient time for it to breakdown even when operating in plasma of density 10^{14} ions/cc, yet enough to cover the microsecond duration of the beam.

U.K.A.E.A. Research Group,
Culham Laboratory,
Nr. Abingdon,
Berks

October, 1964 (C/18 IMG)

CONTENTS

INTRODUCTION

1. The methods described in this report have been used to detect and measure an electron beam circulating in a toroidal plasma. The measurements were made in the course of an experiment to determine the interaction of an electron beam with a toroidal plasma in a magnetic field for which only preliminary results have been given so far[1]. Further results, together with a description of the electron gun used and detailed measurements of the electron beam trajectory around the torus are given in the supporting paper[2] and reports[3,4].

2. The velocity of the electron beam was directed mainly along the magnetic field lines and was about two orders of magnitude greater than the random electron velocities in the plasma. However, in the experiments the density of plasma electrons could be as much as four orders of magnitude more abundant than the beam electrons. It follows that the means of detection must use properties of the electrons which vary sufficiently steeply with velocity to outweigh the small density.

3. The quantities we have been concerned to measure are the flux and the distributions in space and energy of the beam after it has travelled different distances around the torus in the plasma. We wished to determine how these quantities depend on the properties of the plasma; its density and temperature, and on the confining magnetic field. Since there are no ends to the apparatus these measurements were made entirely in the plasma. The drift of the beam across the magnetic field due to the curvature, together with a small radial displacement of the field, separated the beam on each circuit and allowed each circuit to be measured independently. The mean circumference of the torus is 380 cms and so the path-length was sufficiently long for the oscillations which constitute the interaction to build up to a limiting value.

METHODS OF DETECTION

SOFT X-RAY ANALYSIS

4. Measurements of X-rays emitted from inserted tungsten targets, and from the torus walls, excited by 'runaway' electrons with energies comparable to those in our electron beam have previously been reported by Gibson[5]. The energy and flux of the 'runaway' electrons have been inferred from these measurements[6]. We have used an adaptation of this method to measure the intensity and energy of the injected electron beam.

5. We begin by some practical considerations of the X-ray flux expected. The intensity

distribution of the continuous X-ray spectrum has been measured by Dyson[7] for some metal targets bombarded by monoenergetic electrons with energies below 10 keV. The energy intensity of the emitted quanta falls off linearly with their energy, reaching zero when this energy is equal to that of the bombarding electrons. The total energy conversion efficiency μ is given approximately by:-

$$\mu = 1.3 \times 10^{-9} \, Z V_o \, , \qquad \ldots (1)$$

where Z is the atomic number of the target metal, and V_o is the voltage of a monoenergetic electron beam. The number, dn, of quanta, whose energy is between V and $V + dV$ electron volts, emitted from a tungsten target ($Z = 74$) when it is bombarded by N electrons with voltage V_o is given by the distribution

$$dn = 1.9 \times 10^{-7} \, N \left(\frac{V_o}{V} - 1 \right) dV \, . \qquad \ldots (2)$$

We used scintillation detectors with plastic phosphors (NE 102) the light output of which is proportional to the energy of the quanta deposited in the phosphor[8]. Different thicknesses of beryllium and aluminium foil filtered the X-rays and gave different effective energy thresholds V_c for quanta to reach the phosphor.

6. If a fraction α of the electrons strike a mesh target and a fraction β of the quanta emitted are detected due to geometrical considerations then the output signal S of the detector is given by

$$S = k \, \alpha \, \beta \int_{V_c}^{V_o} eV \, dn \, . \qquad \ldots (3)$$

The fluctuation in the number of quanta detected is given by the Poisson distribution and is $\pm \, (\alpha\beta \, dn)^{\frac{1}{2}}$ for the range of energy V to $V + dV$. The signal fluctuation ΔS will be the statistical sum of the associated fluctuations in energy

$$\Delta S = k \sqrt{\alpha \beta \int_{V_c}^{V_o} (eV)^2 \, dn} \, . \qquad \ldots (4)$$

Thus the signal to noise ratio r, i.e. $\left| \frac{S}{\Delta S} \right|$, is

$$r = (1.9 \times 10^7 \, N \alpha \beta)^{\frac{1}{2}} \frac{\int_{V_c}^{V_o} (V_o - V) \, dV}{\int_{V_c}^{V_o} V(V_o - V) dV} \, ,$$

or

$$r = 7.6 \times 10^{-4} \left\{ N \alpha \beta \left(\frac{V_o/V_c - 1}{V_o/V_c + 2} \right) \right\}^{\frac{1}{2}} \, . \qquad \ldots (5)$$

For a shot to shot variation in signal of less than $1/r$ the total charge Q is given by

$$Q = Ne > 2.8 \times 10^{-13} \frac{r^2}{\alpha\beta} \left(\frac{V_o/V_c + 2}{V_o/V_c + 1} \right) \text{ coulombs} \, . \qquad \ldots (6)$$

With $r = 10$, a 10% variation; $\alpha = 0.2$; $\beta = 10^{-4}$; $V_o = 5$ keV and $V_c = 1$ keV, we have

$$Q > 2.5 \times 10^{-6} \text{ coulombs.} \qquad \ldots (7)$$

We see that for an electron beam of as long as one microsecond duration the current would have to be 2.5 amps to give only a 10 per cent shot to shot variation.

7. Initially it was proposed to use a tungsten wire mesh target spread over the complete torus bore to sample 20 per cent of the beam per revolution. It was hoped that, provided the beam was short enough (say half the distance round the torus), we could get information about the beam velocity and velocity dispersion each revolution from the time variations of the X-ray bursts. Alternatively if the degradation of the beam took many circuits to become appreciable then the beam duration could be that much longer.

8. The electron gun had a maximum perveance of 2.0×10^{-6} amps volts$^{-3/2}$ which gives a current of 0.7 amps at a voltage of 5 kV. Therefore, the beam duration, or resolution time, would have to be at least 3 microseconds to satisfy equation (7) and correspondingly more by the number of observations required. Experimentally we found that the beam is only contained in the torus for some ten circuits[4] which is a time of just under a microsecond. Therefore, there just is not sufficient time to make measurements with this system.

9. It is, however, possible to collect all the beam on a solid target after it has travelled a known distance round the torus by using a target of the right shape in the right place. This can be determined by measuring the trajectory of the beam in the magnetic field[4]. Since all the beam is collected ($\alpha = 1$) and only one observation is made, a shot to shot variation of less than 10 per cent is obtained with a beam duration greater than 0.7 microseconds. The beam duration was 1 microsecond in the experiments.

10. When the beam is not monochromatic then let

$$dN = f(V_o)\, dV_o \,, \qquad \ldots (8)$$

where $f(V_o)$ is the distribution function of the beam. We assume $f(V_o) \neq 0$ for $V_m > V_o > V_c$ where the maximum beam energy is V_m and the beam does not spread below the cut-off energy V_c. The signal 'S' from combining equation (3) with (8) and (2) now becomes

$$S = 1.9 \times 10^{-7}\, k\, \alpha\beta \int_{V_c}^{V_m} \left[\int_{V_c}^{V_o} eV \left(\frac{V_o}{V} - 1 \right) dV \right] f(V_o)\, dV_o \,. \qquad \ldots (9)$$

If N is the total number of electrons striking the target, $\bar{V}$ is the mean energy in electron volts and σ^2 is the mean square spread of this energy, then we have:

$$N = \int_{V_c}^{V_m} f(V_o)\, dV \ , \qquad \ldots (10)$$

$$\bar{V} = \int_{V_c}^{V_m} V f(V_o)\, dV \ , \qquad \ldots (11)$$

$$\sigma^2 = \int_{V_c}^{V_m} (\bar{V} - V)^2 \, f(V_o)\, dV \ . \qquad \ldots (12)$$

In terms of this notation it is easily shown that equation (9) becomes

$$S = \frac{1.9 \times 10^{-7}}{2} \, k \, \alpha\beta \, Q \cdot \left\{ \left(\bar{V} - V_c \right)^2 + \sigma^2 \right\} . \qquad \ldots (13)$$

We therefore see that for a given charge and mean energy, that 'S' will increase if the beam energy spreads. In fact 'S' may still increase if the spread is great enough even though $\bar{V}$ decreases. If R is the ratio of the signal 'S' to its initial value for a monochromatic beam injected with energy V_o, then

$$R = \frac{(\bar{V} - V_c)^2 + \sigma^2}{(V_o - V_c)^2} \qquad \ldots (14)$$

From two such ratio's R_1 and R_2 for scintillation detectors with V_c respectively V_1 and V_2 we have:

$$\bar{V} = \frac{1}{2} \left\{ \frac{R_1(V_o - V_1)^2 - R_2(V_o - V_2)^2}{V_2 - V_1} + V_2 + V_1 \right\} , \qquad \ldots (15)$$

$$\sigma^2 = R_1(V_o - V_1)^2 - (\bar{V} - V_1)^2 \qquad \ldots (16)$$

Equations (15) and (16) are true provided the incident charge 'Q' is constant and the spread does not extend beyond the highest threshold V_c ; i.e. $\sigma^2 < (\bar{V} - V_c)^2$.

11. The ratio $\frac{S1}{S2}$ is independent of the charge Q and if, also, $\sigma^2 \ll (\bar{V} - V_c)^2$, it depends only on the mean energy $\bar{V}$. Under these conditions this can be a useful method of determining $\bar{V}$ from the ratio $\frac{S2}{S1}$. If all the dependent parameters vary it is necessary to have three signals, S1, S2 and S3 with different thresholds V1, V2 and V3 to evaluate the unknowns Q, V and σ. The method now become rather unwieldy to use.

ACCURACY OF MEASUREMENT

12. The signal S increases with spread therefore the lowest signal-to-noise ratio r_{min} occurs for $\sigma = 0$. For a beam with perveance 'p', accelerating voltage 'V_g' and duration 't' seconds, we obtained from equation (5)

$$r_{min} = 7.4 \times 10^{-4} \left\{ \alpha\beta \, \frac{p V_g^{3/2} t}{e} \, \frac{\bar{V}/V_c - 1}{\bar{V}/V_c + 2} \right\}^{1/2} . \qquad \ldots (17)$$

Typically $V_g = 5$ keV; $t = 10^{-6}$ secs; $\alpha = 1$; $\beta = 10^{-4}$; $\bar{V}/V_c > 2$; and $p = 2.0 \times 10^{-6}$ so that $r_{min} \sim 8$. In order to obtain sufficient accuracy with this method it is necessary to average over many results.

APPRAISAL OF THE X-RAY METHOD

13. The poor conversion efficiency found in the X-ray method which necessitates averaging over many results can be balanced against the following advantages. The method is simple and requires only a tungsten target of the right dimensions immersed in the plasma at the required place. The measurements are practically independent of the distribution of energy along and perpendicular to the field lines and depend only on the total energy. The beam is affected a minimum amount by the measurements. Only a very small fraction of the incident primary electrons are returned up the path of the beam. These are a possible source of 'feed back' oscillations. For instance an analyser using a retarding potential which we now describe has been observed to move the beam to a different position.

RETARDING POTENTIAL ANALYSER

14. This method has been used to measure both the space and energy distribution of the electron beam in vacuum, in neutral gas and in the presence of plasma. The retarding potentials are applied parallel to the axis of the beam that is along the direction of the magnetic field. Therefore, only the component of electron momentum parallel to the field is effective in overcoming this potential. The aperture of the analyser depends on the perpendicular component of energy.

15. The analyser is shown schematically in Fig.1(a). The beam enters through grid (1)

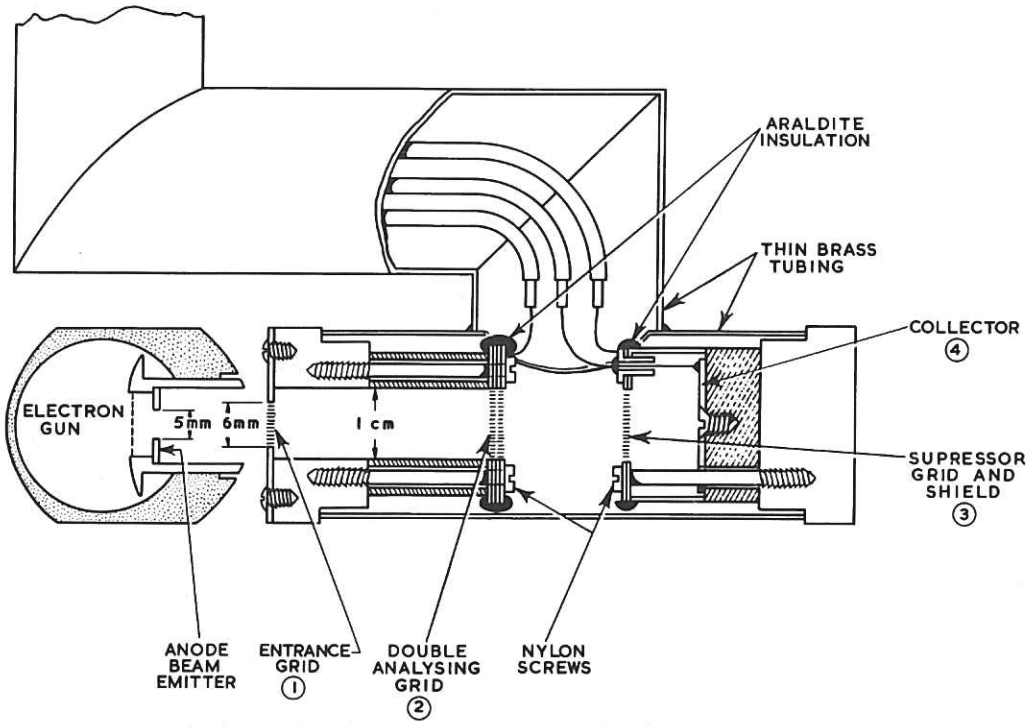

Fig. 1(a) Retarding potential analyser (CLM-R 39)

and passes down a tunnel whose bore is the order of the Larmor diameter of the electrons, if all their energy were directed perpendicular to the field, and whose length is sufficient to give at least one Larmor period during the transit within the tunnel, if all the electron energy was directed along the field lines. The tunnel aperture decreases linearly with the perpendicular electron energy and reaches zero when this is 8 keV at 600 gauss, and 22 keV at 1000 gauss. The maximum beam energy is 8 keV so with a weak magnetic field it is possible that those incident electrons cannot enter which have all their energy transverse to this field.

16. The entrance aperture is made constant for electrons with perpendicular energies up to ¼ of these limits, by restricting the size of the aperture at grid (1) to ½ the radius of the tunnel.

17. Grid (2) is the analysing grid. Electrons are reflected back when their parallel energy is not sufficient to overcome the potential on this grid. It is a double grid to increase the resolution to a fraction of a per cent and yet have a good transmission factor, 72%. This grid also collects any positive ions that may come into the system from the plasma. Its potential may be pulsed on for periods of a few microseconds, up to voltages of 8 kV. The analyser can be immersed in a plasma of 10^{14} electrons per cc. without this potential breaking down. It may also be operated with static potentials of this magnitude at pressures up to a few hundred microns of neutral hydrogen gas.

18. Grid (3) forms part of the electrostatic shield around the collector (4). It is held at 60 volts negative to the collector in order to suppress secondary electrons from it. Grid (3) is decoupled to earth through a condenser so that there is little effect on (4) when the voltage on (2) is pulsed on and off. The collector voltage differs from earth by only the signal voltage of the collector current passing through the measuring circuit. All the grids used are 85% transmitting. Thus the collector current is 52% of the beam current.

19. The collector current, I_C, is fed directly to the oscilloscope where it can be displayed as a voltage signal across the appropriate terminating resistor for the connecting cable, in which case the response is only limited by the rise time of the amplifiers in the oscilloscope (12 milli-microseconds). Otherwise it may be integrated across a simple resistance capacity network. The oscilloscope then shows the total charge of the beam collected, 'Q'.

20. We plot 'Q' for different retarding potentials 'V_r' applied to grid (2). The slope

from this graph $\frac{dQ}{dV_r}$ gives the average energy distribution of the beam. Similarly the average beam profile in space can be plotted for various retarding potentials by moving the analyser, and plotting 'Q' against the coordinates (x, y) of the analyser within the torus bore.

21. The direct signal can also be used to show the time variations in the collector current against both position (x, y) and retarding potential 'V_r'. This signal was similar to the accelerating voltage pulse V_g applied to the gun only for the initially injected beam. For tractable results we therefore required the retarding potential 'V_r' in the form of a square wave of variable amplitude, switched on before the beam pulse and lasting a microsecond longer. Fig.1(b) shows the Blumlien circuit used to produce this pulse which lasted for two microseconds. It is very similar to that used for the electron gun pulse[3], except that a spark gap is used to initiate the pulse. This proved to be a more efficient delay line switch and gave an improved waveform.

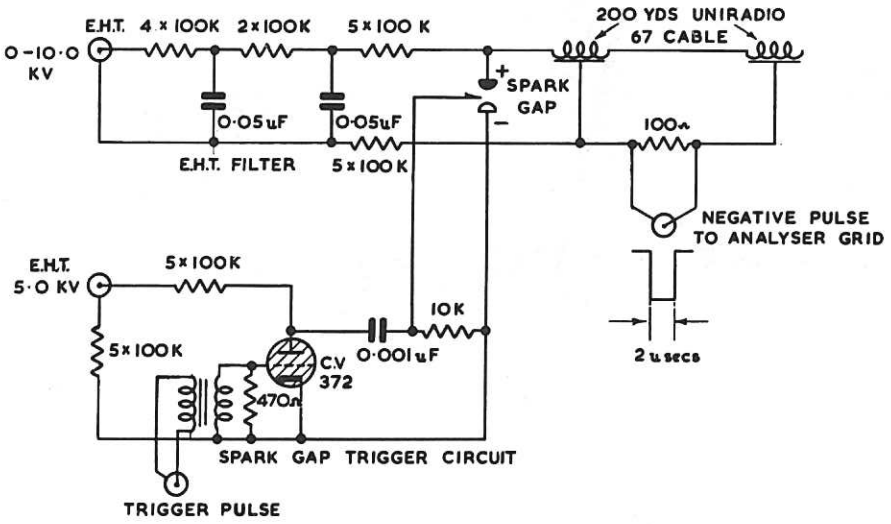

Fig. 1(b) Blumlein circuit - 2.0 μs pulser (CLM-R39)

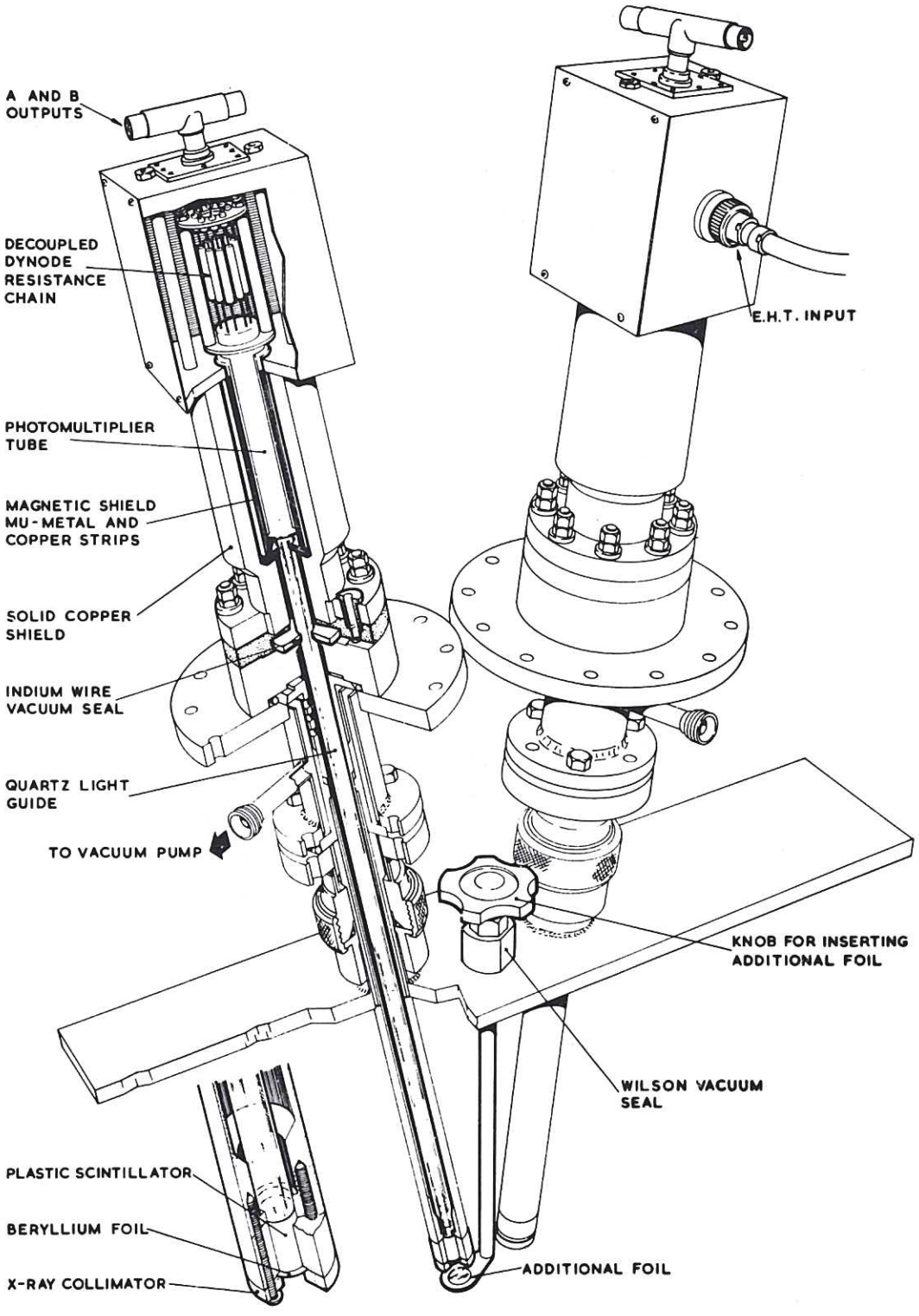

Fig. 2 X-ray scintillation detector system (CLM-R 39)

EXPERIMENTS

22. To illustrate the methods used, we now give some experimental calibrations and results, although the results are given in detail in the supporting paper[2]. Fig.2 is an illustration of the scintillation detectors used. The design is similar to that used by Gibson and Mason[6]. X-rays were filtered by a thin beryllium foil; thicknesses of from 0.001 inch to 0.006 inch were used to give threshold energies of from 1 to 2 keV. We used a plastic phosphor (type N.E.102), manufactured by Nuclear Enterprises, which was 0.6 inch thick. A quartz guide conveyed the phosphorescence to a photomultiplier tube (E.M.I. type 9526). The signal was directly fed from the photomultiplier to the oscilloscope (Tektronix type 555). Fig.3 shows the circuit. We had the choice of a direct signal A taken from a dynode chain, or an integrated signal B from the anode. In most of the experiments B only was used. The time constant was some hundreds of microseconds so the whole X-ray burst was integrated. A was used for testing and setting up. The transit time spread was 18 millimicroseconds. From A together with a direct signal B' from the anode we

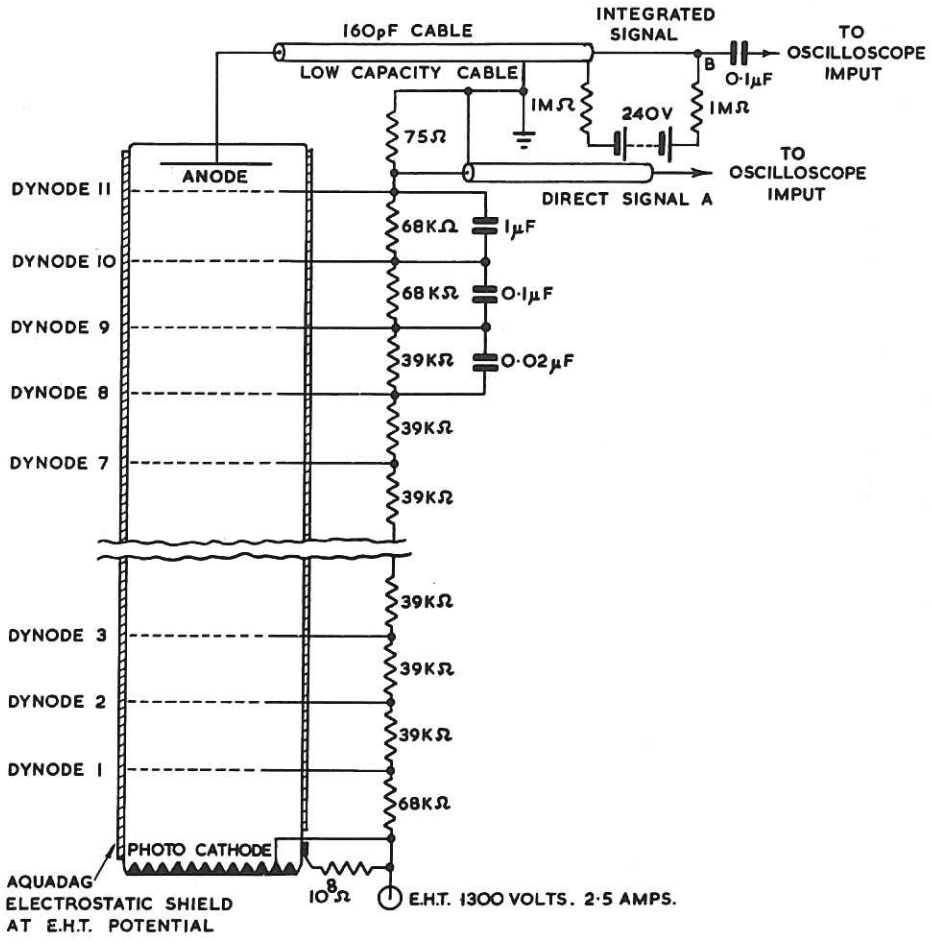

Fig. 3 Photomultiplier circuit (CLM-R39)

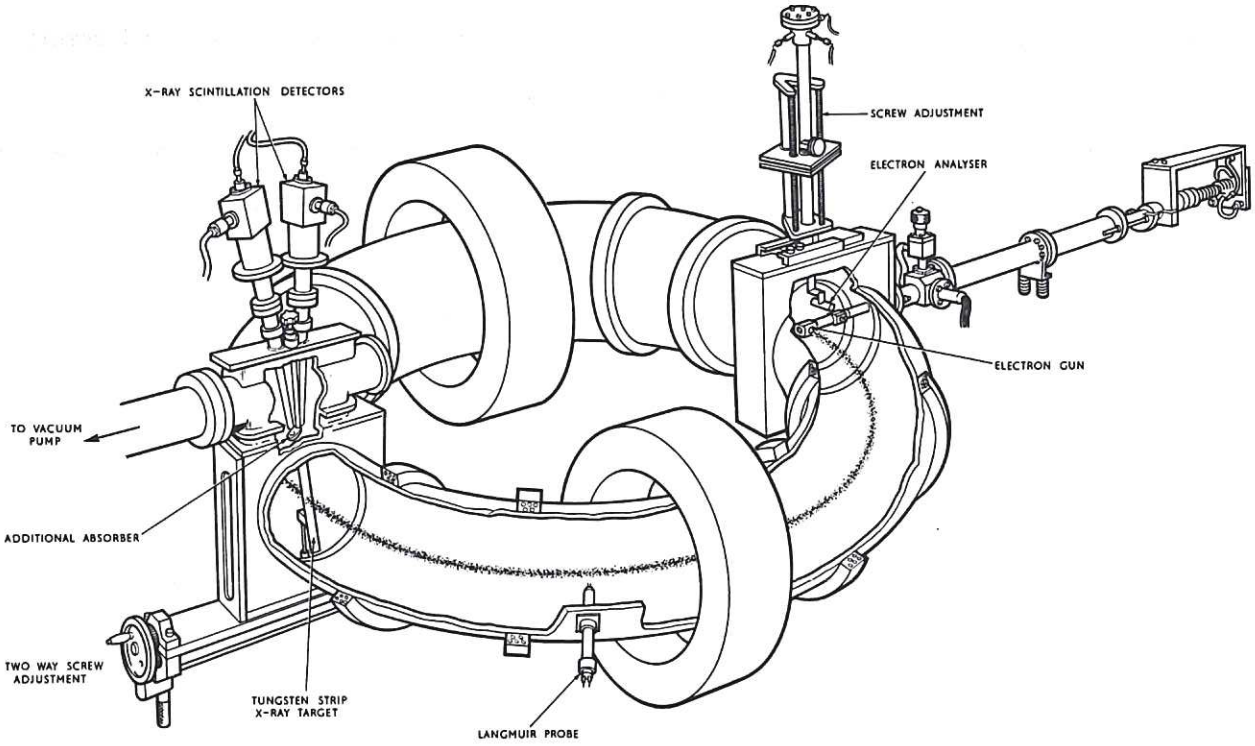

Fig. 4 Experimental set-up on Mark IV torus (CLM-R39)

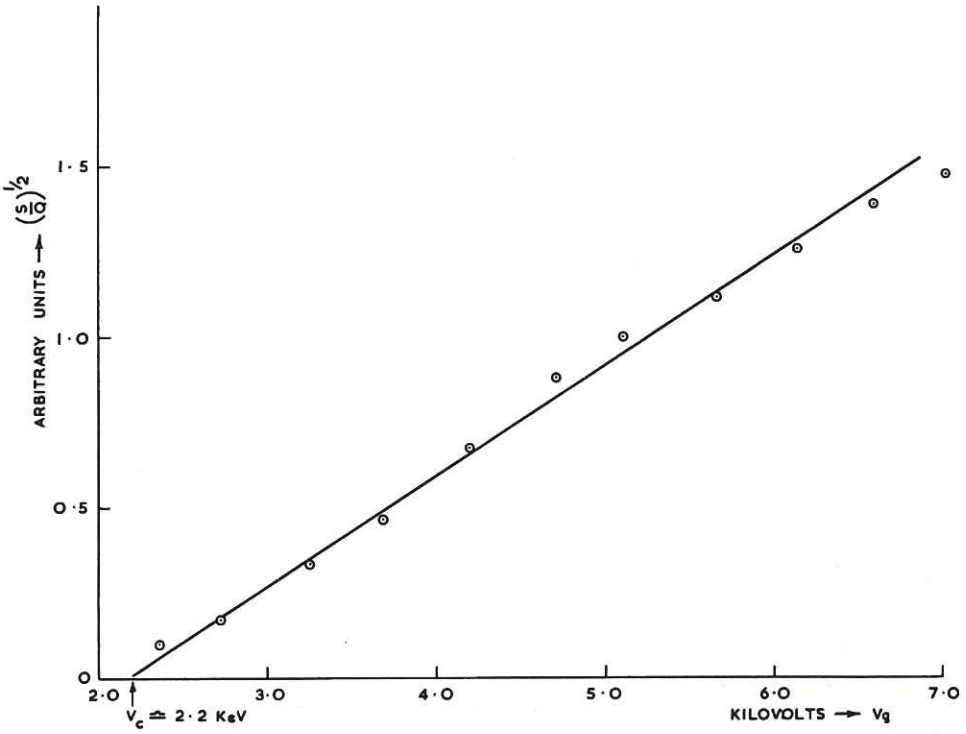

Fig. 5 Calibration plot of 0.005 inch Be foil (CLM-R39)

would also obtain a balanced output which eliminated interference. Fig.4 shows the set-up used in the majority of the experiments. A method for providing a third signal, with threshold V_3 lying between V_1 and V_2, by means of a separate additional foil, which can be swung into place, is shown.

23. Absorption coefficients vary very rapidly with X-ray energy[9] and because of this, the threshold is relatively sharp. We have computed the thresholds for various thicknesses of beryllium and also for the plastic scintillator itself, which must stop all the X-rays. These values are consistent with what we find experimentally. Fig.5 shows a typical plot obtained from calibrating a 0.005 inch foil in vacuum. The electron beam was fired with a measured pulsed voltage V_g on the gun. It was guided round the torus by a confining magnetic field and half way round, a distance of 191 cms, it struck tungsten target. This was kept 20 volts positive with the respect to the torus liners during calibration, to prevent loss of secondary electrons. The charge collected, Q, was measured by integrating the current. We plot the function $\left(\frac{S}{Q}\right)^{\frac{1}{2}}$ in arbitrary units, where S is the time integrated scintillator signal against V_g in kilovolts. A fairly good straight line is obtained up to energies of 7 kV on the beam, and this extrapolates to cut the voltage axis at the threshold; V_c = 2.2 kV.

24. Using two scintillation detectors with thresholds energies $V_1 = 0.9$ keV and $V_2 = 2.2$ keV we can obtain the ratios $\frac{S_2}{S_1}$ as a function of the initial beam voltage V_g. This is plotted in Fig.6, curve (i). Curve (ii) of this figure is the ratio for the case where the beam

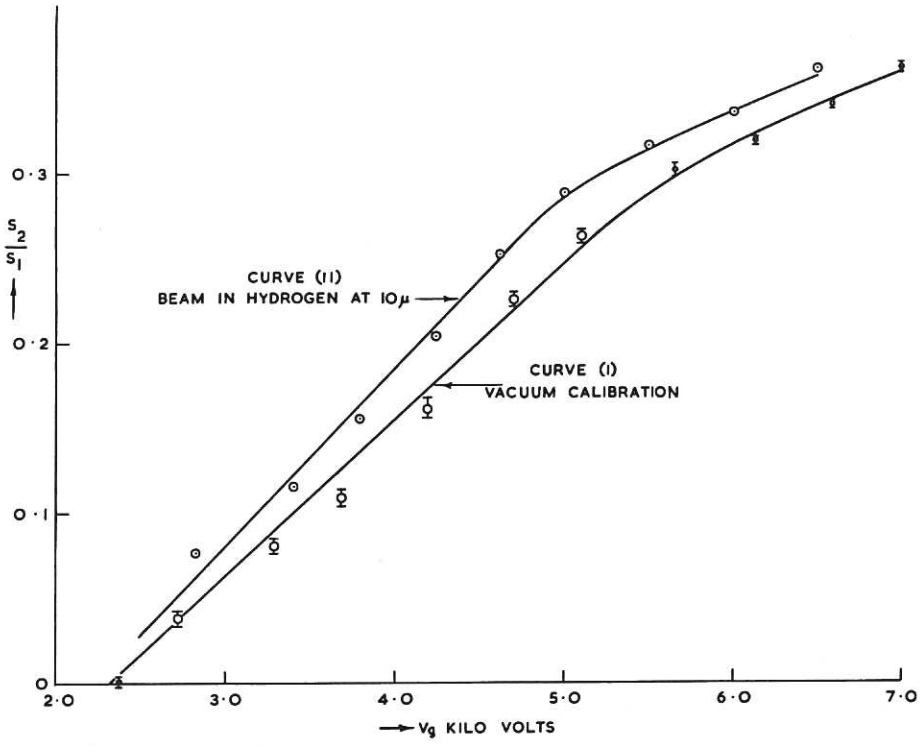

Fig. 6 Ratio $\frac{S_2}{S_1}$ of scintillation signals after half circuit of torus (CLM-R39)

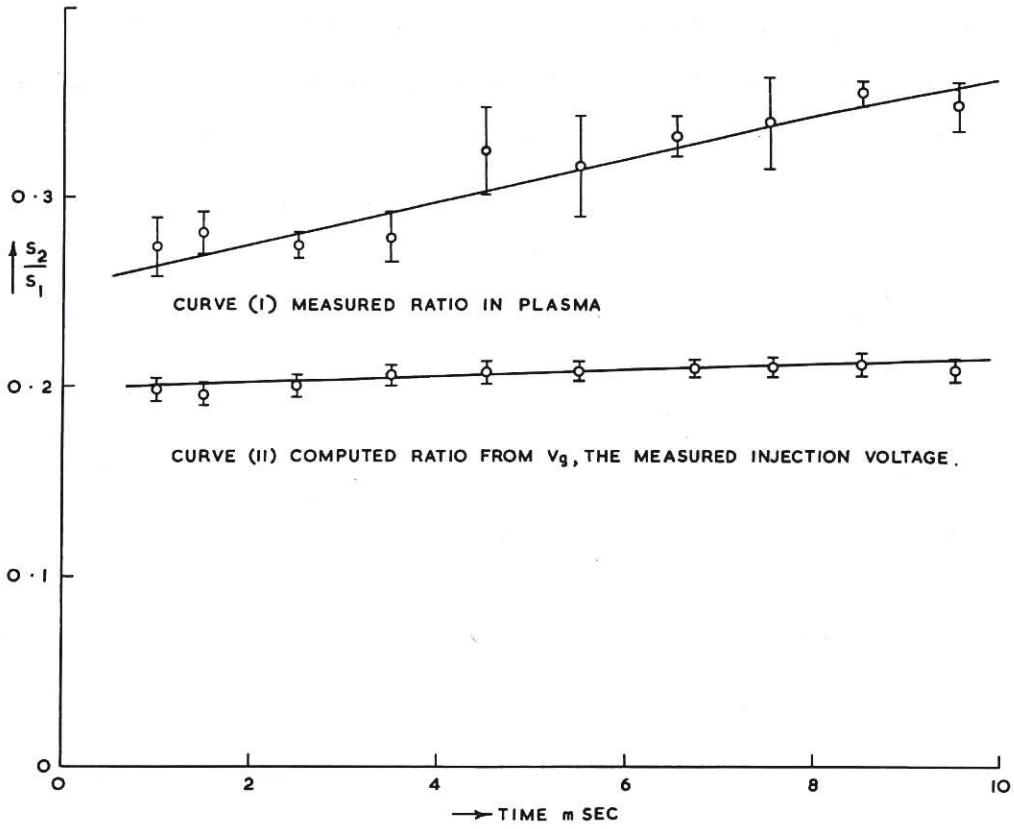

Fig. 7 Ratio $\frac{S_2}{S_1}$ after half circuit in plasma (CLM-R 39)

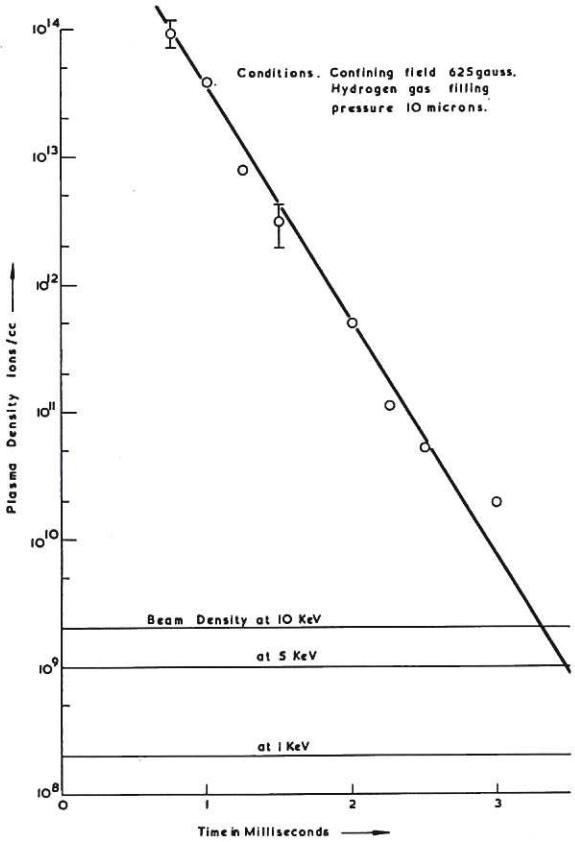

Fig. 8(a) Plasma density variation with time (CLM-R 39)

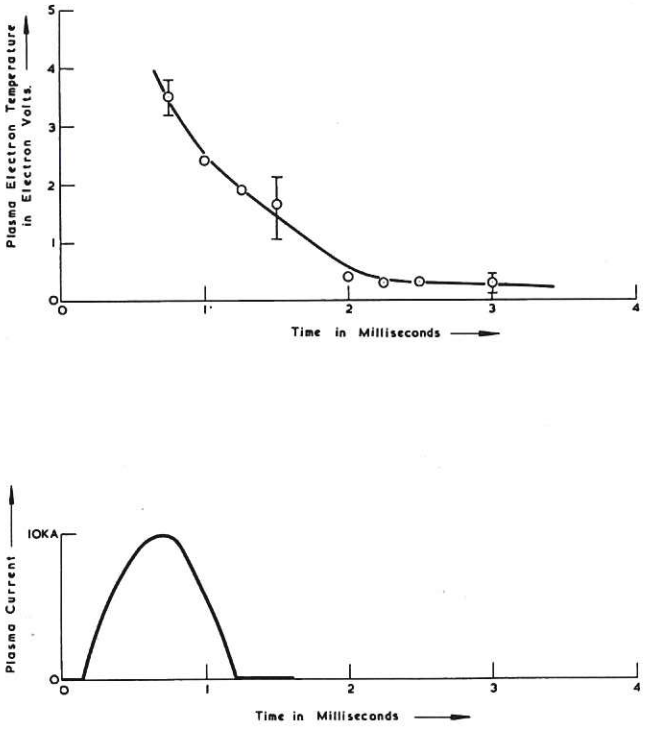

Fig. 8(b) Variation of plasma temperature and current with time (CLM-R 39)

has travelled through hydrogen gas at a pressure of 10 mTorr. The values for this ratio are consistently higher than those, for the same V_g, in vacuum, by the equivalent of ~400 volts.

25. Ratios taken when the beam has penetrated through an afterglow plasma whose density is exponentially decreasing with time are shown in Fig.7 as a function of time, for a beam injected with $V_g = 4.5$ to 4.6 kV. Fig.8 shows the variation of the relevant plasma parameters, electron density and temperature and gas current, as a function of time. The mean confining field was 620 gauss and the starting pressure 10 mTorr of hydrogen. We see that the ratios are higher still. We show in the appendix that, for this ratio to increase, we must have at least some electrons with energies greater than those we injected. Therefore, even if the calibrating beam already has an appreciable energy spread on injection, it is not possible, by binary collisions with neutral gas molecules alone, for this measured ratio to increase. These collisions, although they could preferentially remove the slower electrons to energies where they are not measured by the scintillators (energies less than the threshold) yet cannot form electrons with greater energy than before. Here we note that the mean free path for an ionizing collision in hydrogen increases proportionally to energy if it is above 200 eV and equals the target distance of 191 cms for 2 keV electrons at a pressure of 10 mTorr[10]. The energy lost in each collision is about the ionization energy of 13.6 eV.

26. The energy distribution for the beam as it leaves the gun is measured by the retarding potential analyser and is shown in Fig.9, taken respectively in vacuum (a base pressure of

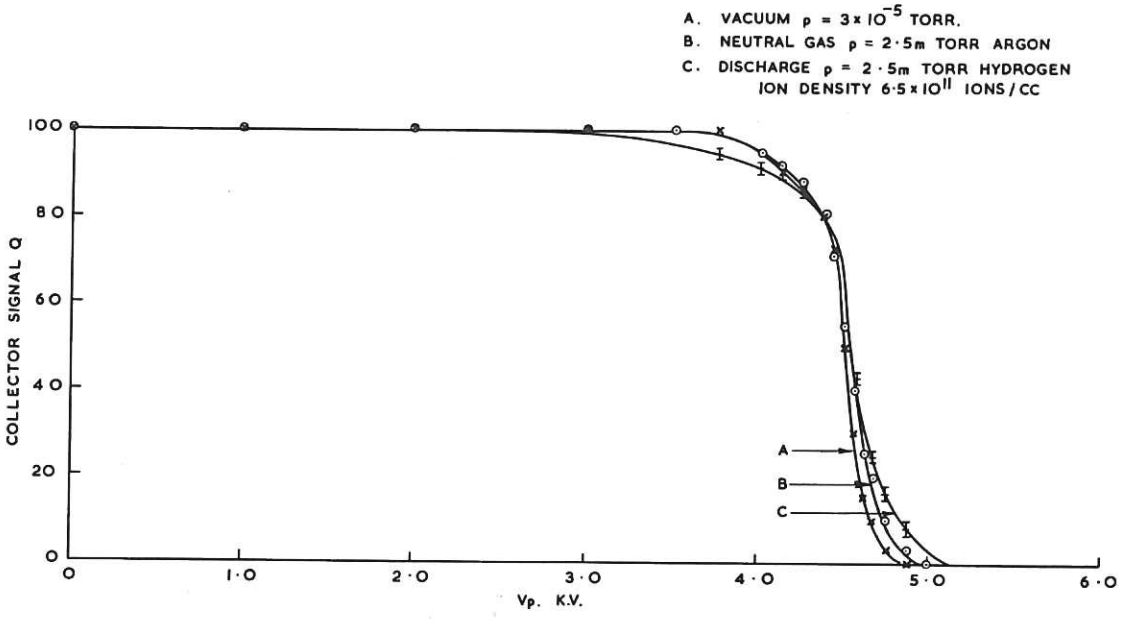

Fig. 9 Bias plot of beam 0.3 cm in front of gun (CLM-R39)

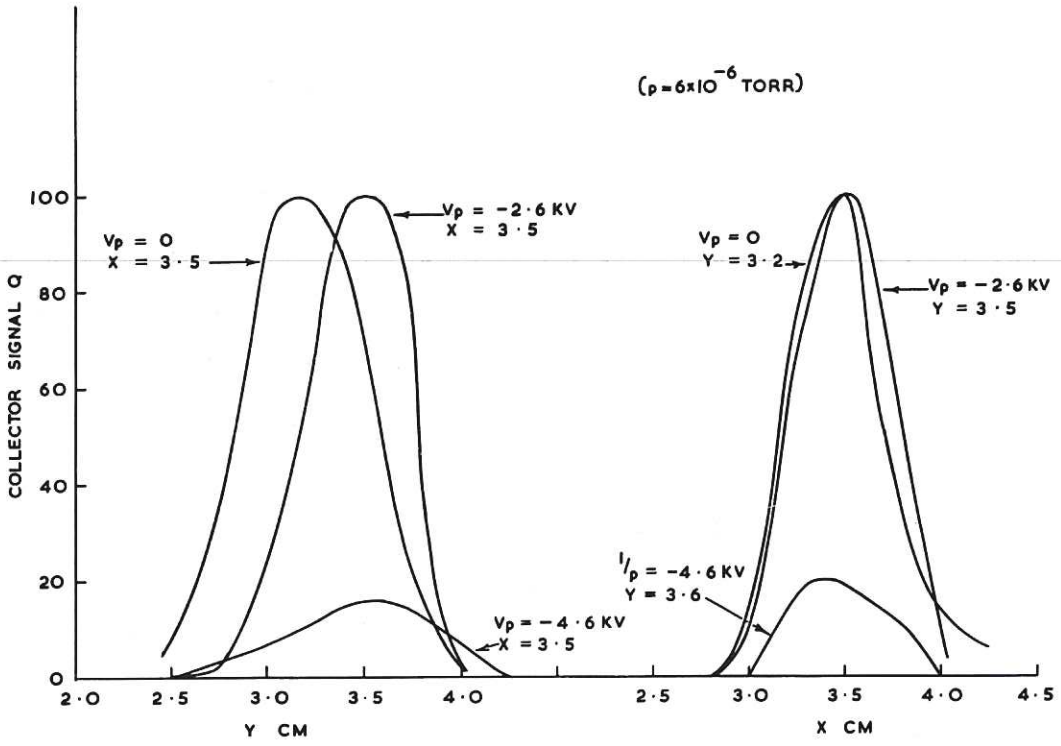

Fig. 10 Spatial profiles of electron beam after 1 circuit in vacuum (CLM-R 39)

10^{-5} Torr), in hydrogen at 2.5 mTorr pressure and in plasma of density 6.5×10^{11} ions/cc. In Fig. 10 we show the beam 'profile' given by the collected charge 'Q' for different positions in x and y respectively, near the centre of the beam after one circuit round the torus. These plots are taken at different values of the retarding potential V_r. We note that the beam centre appears to move vertically (in the direction of increasing y) as the potential V_r is raised. We attribute this to 'feed-back' oscillations excited by electrons, which have failed to be collected, returning along the path of the beam. We may plot from Fig. 10 the electron energy distribution taken at the peaks, corresponding to the beam

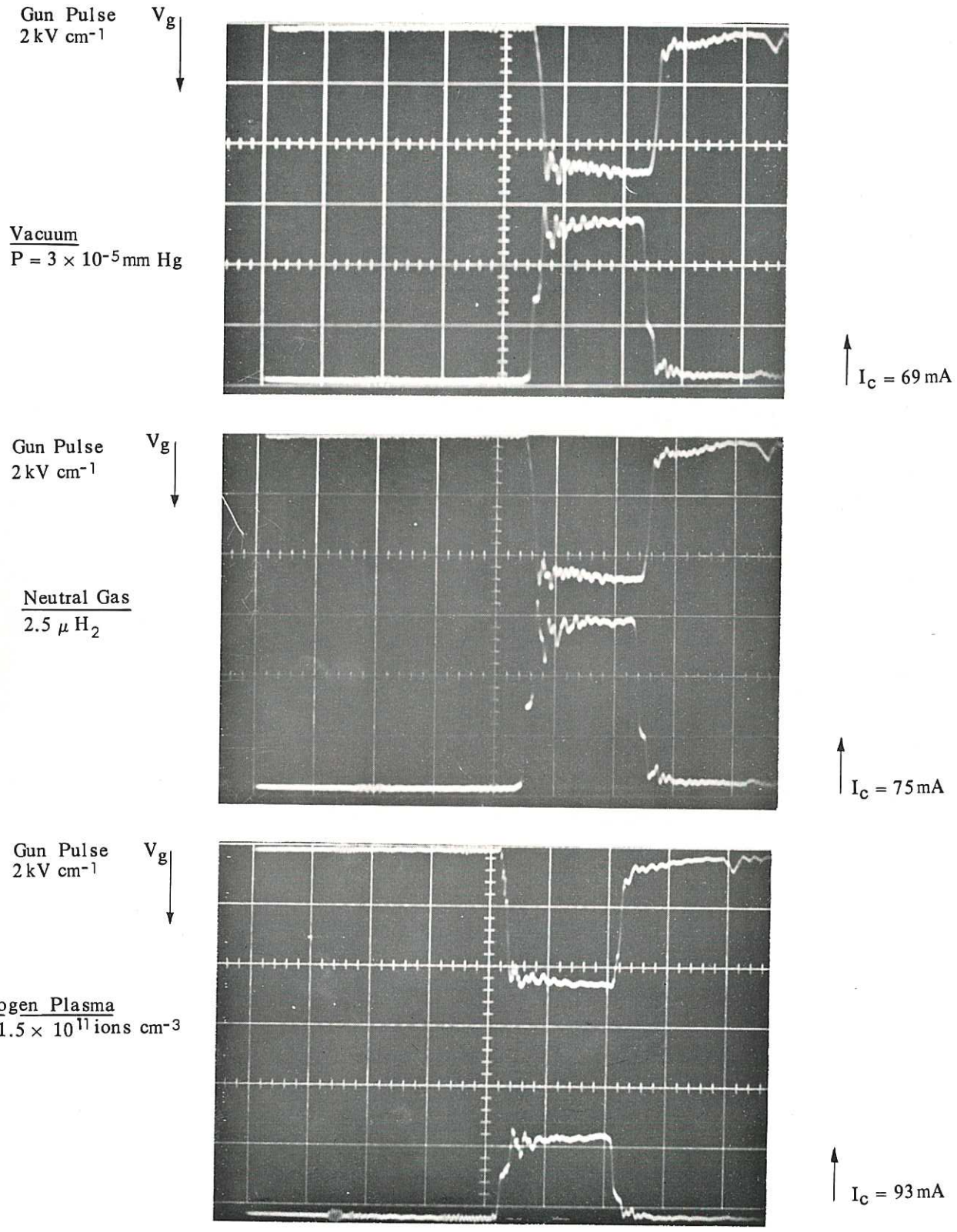

Fig. 11 Electron analyser in front of gun (CLM-R 39)

Operating conditions affect collector current I_c

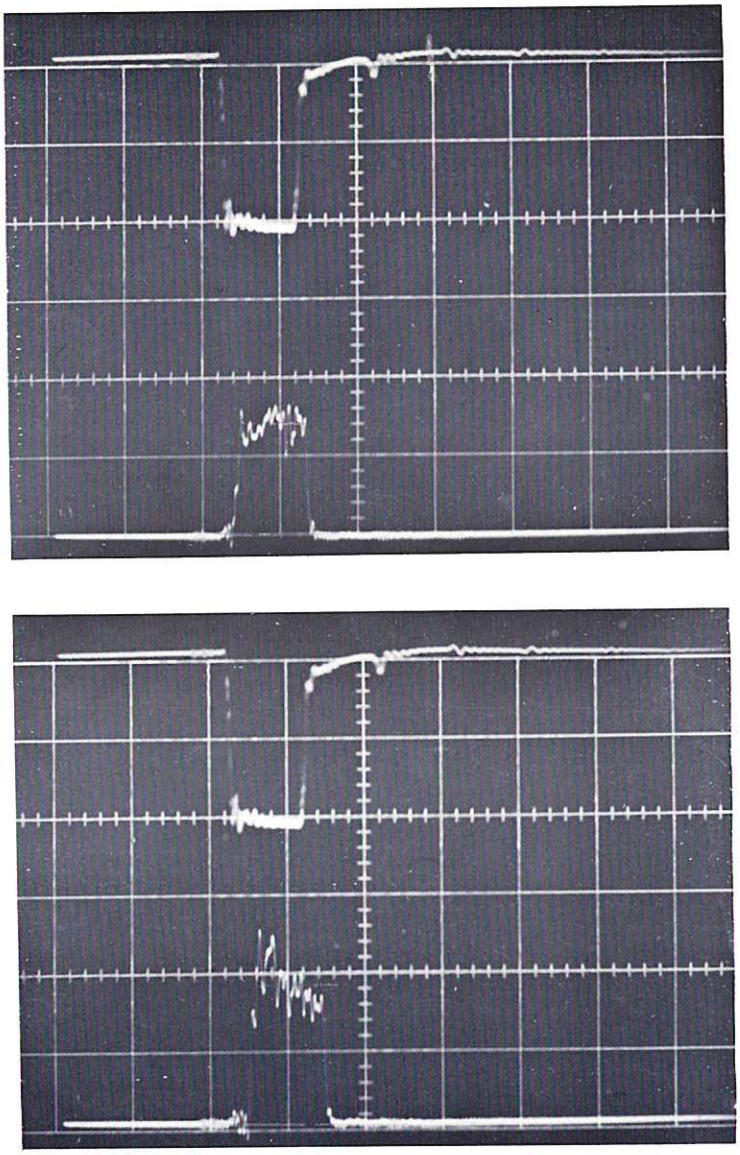

Fig. 12 (CLM-R 39)
Comparison of collector current I_c after one and then after two circuits in a hydrogen plasma, at initial pressure 2.5 mTorr and $N_i = 4 \times 10^{11}$ ions cm^{-3}
Bias $V_p = 0$

centre. Figs.11 and 12 show typical oscillograms of the time variation in collected current taken respectively as the beam leaves the gun and after one complete circuit round the torus.

27. Current fluctuations develop as the beam travels around the torus. The actual position of the beam varies in vacuum, because of the effect of stray fields associated with a neighbouring cyclotron. In the presence of plasma this is shielded out and the fluctuations are smaller. The fluctuations are greatest in neutral hydrogen gas. Little current can be detected when the pressure lies in the range 0.6 to 1.0 mTorr, which may be explained by the fact that an electron beam of 4.4 kV produces in hydrogen its own density of ions after one microsecond when the pressure is about 1 micron. Thus the beam and plasma frequencies are equal so the interaction is strongest.

CONCLUSIONS

28. We have described here two methods which we have used to measure the relevant parameters of an electron beam circulating in a toroidal system with a confining magnetic field. Measurements have been made on the beam circulating in vacuum, in hydrogen gas at pressures up to 10 mTorr, and on the beam immersed in a plasma. We have shown how measurements are made and interpreted. We have been able to demonstrate with these measurements beam instabilities and collective beam plasma interactions. These are reported in detail in the supporting paper[2].

REFERENCES

1. TOSSWIL, C.H., SCHOFIELD, J.M.S. and ATKINSON, D.W. Beam-plasma interaction in a torus. Bull. Amer. Phys. Soc. series II, vol.7, no.2, p.151. February 23, 1962. (Abstract only)

2. ATKINSON, D.W., FRANCIS, G. and SCHOFIELD, J.M.S. The interaction of an electron beam with a plasma in a toroidal magnetic field. J. Nucl. Energy. Pt C. (To be published).

3. ATKINSON, D.W. and SCHOFIELD, J.M.S. An electron gun designed to operate totally immersed in high density plasma. (To be published)

4. ATKINSON, D.W. and SCHOFIELD, J.M.S. Experimental determination of the displacement per revolution of the applied magnetic field in the Mk IV Torus using an electron beam. CLM-M 38. November, 1964.

5. GIBSON, A., Runaway electrons. Third International Conference on Ionization Phenomena in Gases, Venice, 1957. Proceedings, pp.365-398, October 1957.

6. GIBSON, A. and MASON, D.W. Energy loss processes in ZETA. Proc. Phys. Soc., vol.79, pt 2, no.508, pp.326-350, February, 1962.

7. DYSON, N.A. The continuous x-ray spectrum from electron-opaque targets. Proc. Phys. Soc., vol.73, pt.6, no.474, pp.924-936, June, 1959.

8. MEYEROTT, A.J., FISHER, P.C. and ROETHIG, D.T. Plastic scintillator response to 1-10 keV photons. Rev. Sci. Inst. vol.35, no.6, pp.669-672, June, 1964.

9. COMPTON, A.H., and ALLISON, S.K. X-rays in theory and experiment. 2nd ed. Princeton, Van Nostrand, 1935.

10. VON ENGEL, A. Ionized gases. p.52, Oxford, Clarendon Press, 1955.

APPENDIX

29. We show that the distribution function $f(V_o)$ must spread to higher energies than V_g, the voltage of the calibrating beam, if the corresponding ratio is greater than the calibrated value, i.e. $f(V_o) \neq 0$ for all $V_o > V_g$. Since the measured ratio is greater than the calibrated ratio we obtain from equation (9):-

$$\frac{S_2}{S_1} = \frac{\int_{V_2}^{V_m} (V_o - V_2)^2 \, f(V_o) \, dV_o}{\int_{V_1}^{V_m} (V_o - V_1)^2 \, f(V_o) \, dV_o} > \left(\frac{V_g - V_2}{V_g - V_1} \right)^2 , \qquad \ldots (A1)$$

or

$$\int_{V_2}^{V_m} \left(\frac{V_o - V_2}{V_g - V_2} \right)^2 f(V_o) \, dV_o > \int_{V_1}^{V_2} \left(\frac{V_o - V_1}{V_g - V_1} \right)^2 f(V_o) dV_o \, . \qquad \ldots (A2)$$

Since $V_g > V_2 > V_1$ (an initial condition)

$$\int_{V_2}^{V_m} \left\{ \left(\frac{V_o - V_2}{V_g - V_2} \right)^2 - \left(\frac{V_o - V_1}{V_g - V_1} \right)^2 \right\} f(V_o) \, dV_o > \int_{V_1}^{V_2} \left(\frac{V_o - V_1}{V_g - V_1} \right)^2 f(V_o) dV_o > 0 , \qquad \ldots (A3)$$

and since $f(V_o) \geqslant 0$, then

$$\left(\frac{V_o - V_2}{V_g - V_2} \right)^2 - \left(\frac{V_o - V_1}{V_g - V_1} \right)^2 > 0 , \qquad \ldots (A4)$$

for some V_o for which $f(V_o) > 0$.

So, since none of the difference terms can be negative because the detectors are insensitive for energies below the corresponding thresholds,

$$\left(\frac{V_o - V_2}{V_g - V_2} \right) - \left(\frac{V_o - V_1}{V_g - V_1} \right) > 0 \qquad \ldots (A5)$$

or

$$\frac{(V_o - V_g)(V_2 - V_1)}{(V_g - V_2)(V_g - V_1)} > 0 , \qquad \ldots (A6)$$

Since all the terms are positive other than $(V_o - V_g)$ we must have this positive also for the inequality to hold. Thus, from (A4), $f(V_o)$ must be non-zero for some $V_o > V_g$. The distribution function must overlap V_g by a significant amount.

Available from
HER MAJESTY'S STATIONERY OFFICE
York House, Kingsway, London W.C. 2
423 Oxford Street, London W. 1
13a Castle Street, Edinburgh 2
109 St. Mary Street, Cardiff
39 King Street, Manchester 2
50 Fairfax Street, Bristol 1
35 Smallbrook, Ringway, Birmingham 5
80 Chichester Street, Belfast
or through any bookseller.

Printed in England

S.O. Code No. 91-3-16-91